Analysis and Design of Circular Prestressed Concrete Storage Tanks

M. J. N. Priestley
Reader in Civil Engineering
University of Canterbury
Christchurch, New Zealand

Prestressed concrete circular tanks are widely used as water supply reservoirs, sewage digesters, and for storage of such diverse materials as acid, oil, cement, hot effluent from pulp and paper factories, and other applications.

Most tanks are cylindrical and ground supported but elevated tanks are used for water supply in areas where local topography is not suitable for natural provision of adequate head for town supply, or where industrial requirements demand short-term provision of large quantities of high pressure water. Such tanks are visually prominent, and aesthetic considerations frequently dictate that more complex shapes than simple elevated cylinders be utilized.

Analysis of cylindrical tanks under axisymmetric loads, such as fluid or gas pressure, is covered by standard texts on the design of circular reservoirs, and is only briefly summarized here. Loads are carried by two contributing mechanisms: hoop stress and bending of the wall along the surface generators. Fig. 1 illustrates the radial deflection of a pinned-base ground supported cylindrical tank under internal fluid pressure, and defines the nomenclature to be used hereinafter.

Consideration of compatibility requirements results in the characteristic equation for radial deformation:

$$\frac{d^4y}{dh^4} + \alpha^4 y = \frac{\phi(h)}{K} \qquad (1)$$

where $\phi(h)$ is the loading function [$\phi(h) = \rho g h$ for fluid loading, where ρ is the mass density and g is the acceleration due to gravity], $K = E_c I/(1 - \nu^2)$, $I = t^3/12$, and:

$$\alpha = \sqrt[4]{\frac{(1-\nu^2)}{R^2 t^2}}$$

is the characteristic of the equation, where R is the tank radius, t is the wall thickness, and ν is Poisson's ratio for the concrete.

Eq. (1) has the typical solution:

$$y = PI + \left[e^{\frac{\alpha h}{\sqrt{2}}} \left(A \sin \frac{\alpha h}{\sqrt{2}} + B \cos \frac{\alpha h}{\sqrt{2}} \right) + e^{\frac{-\alpha h}{\sqrt{2}}} \left(C \sin \frac{\alpha h}{\sqrt{2}} + D \cos \frac{\alpha h}{\sqrt{2}} \right) \right] \quad (2)$$

where PI is the load-dependent particular integral, and A, B, C, D are constants of integration dependent on boundary conditions at the wall base and top.

Once Eq. (2) is solved for y, the complete stress distribution in the tank may be calculated as follows:

Hoop Tension

Since circumferential length and radius R are related by the constant 2π, a radial deformation y causes a circumferential length increase of $2\pi y$. The circumferential strain will thus be:

$$\epsilon_h = 2\pi y / 2\pi R = y/R$$

and hence hoop tension stress is given by:

$$f_h = E_c\, y/R$$

where E_c is the concrete modulus of elasticity.

Vertical Bending

From the beam equation, vertical bending moments are found after double differentiation of Eq. (2), as:

$$M_v = \frac{E_c I}{1 - \nu^2} \cdot \frac{d^2 y}{dh^2} \quad (4)$$

If moments have been calculated for unit wall width, then surface bending stresses in the vertical direction can be found from:

$$f_v = \pm M_v \cdot \frac{6}{t^2} \quad (5)$$

Synopsis

Aspects of the analysis and design of prestressed concrete storage tanks are discussed, and a simple analogy for the analysis of circular prestressed tanks is described.

The method, which is suitable for use with small microcomputers, or even the larger programmable calculators, is capable of modelling both cylindrical tanks, and tanks with double curvature under a wide range of loading, including dead load, fluid or gas pressure, thermal load, and prestressing.

The significance of actions often ignored in tank design, including shrinkage and swelling of the walls, creep redistribution of prestress, and thermal effects are examined in some detail.

Comparisons are given between results predicted by the frame analogy and more sophisticated analytical methods for a ground supported cylindrical reservoir, and an elevated doubly curved tank.

Surface Circumferential Stress

Since the loading and structure are both axisymmetric, radial lines connecting points on the inside and outside surfaces of the tank wall must remain radial after application of loading. This effectively means that transverse Poisson's ratio strains from vertical bending moments cannot develop, and in consequence, the wall is in a state of plane strain for vertical bending. Consequently, circumferential Poisson stresses, νf_v, are developed in the walls.

These Poisson stresses are commonly ignored in design, but can be quite significant, particularly when high bending moments develop from base fixity. Final

circumferential stresses at the wall surface are thus:

$$f_c = f_h \pm \nu f_v = \frac{E_c y}{R} \pm \nu \frac{6M_x}{t^2} \quad (6)$$

Solution of Eq. (1) is tedious and unsuitable for design office usage. Consequently, it is common to use design charts or tables, such as those developed by Creasy[1] or Ghali,[2] which typically give vertical bending moment and hoop tension force as functions of the tank shape factor H^2/Rt and fraction of wall height $x = h/H$. Although such tables and charts are extremely useful, they are limited in applicability.

Generally, loading must be either hydrostatic pressure or uniform (gas) pres-

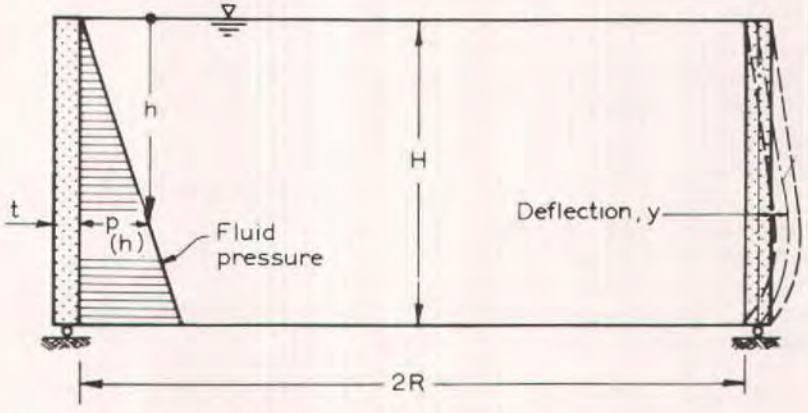

Fig. 1. Pinned-base tank under fluid pressure.

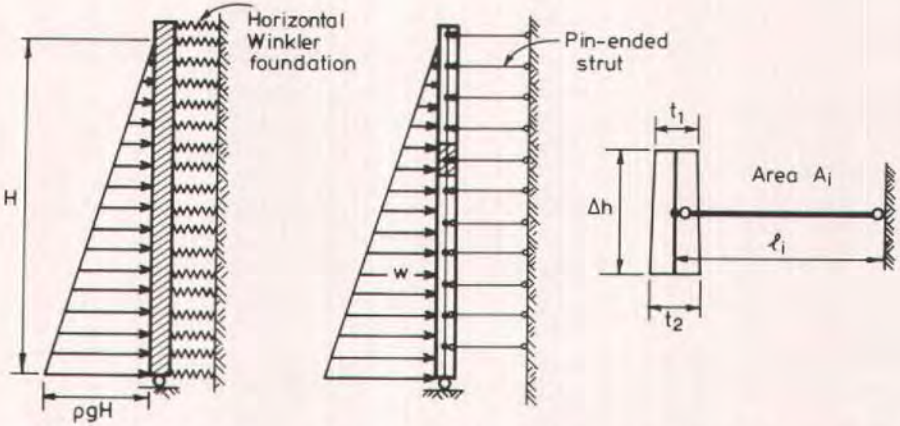

(a) Continuous Winkler Foundation

(b) Discretised Foundation - Frame Analogy

(c) Detail of Equivalent Strut

Fig. 2. Beam on elastic foundation and frame analogy simulations of cylindrical tank wall.

sure over the full height (i.e., partially filled tanks are not considered), or bending moment or shear force applied to top or bottom of the wall. Tank walls must be vertical and generally of uniform thickness, although Ghali[2] includes data for tapering walls.

FRAME ANALOGY

Cylindrical Tanks With Axisymmetric Loading

In the introduction it was established that the response of cylindrical tank walls under rotationally symmetric loads involved load sharing between two mechanisms: hoop tension and vertical bending. Eq. (1) is developed from the compatibility requirement that radial deformations of the two mechanisms must be identical at all points. Behavior can be described as basic vertical beam action, where radial deformations are further constrained by the stiffness of hoop action.

The analogy to Beam on Elastic Foundation (BEF) analysis[3] is obvious, and has been used in the past to generate design tables for tanks. Vertical bending of the tank wall is represented by beam action, and the elastic radial stiffness of hoop action is represented by the spring stiffness of the Winkler[4] foundation.

Consider a unit height of tank wall subjected to pressure p, and freed from cantilever action. From considerations of simple statistics, the radial expansions will be:

$$y = \frac{pR^2}{tE_c} \tag{7}$$

Fig. 2a shows a unit circumferential length of tank wall supported by a horizontal Winkler foundation. Deflection of this foundation under pressure p will be:

$$y = p/k \tag{8}$$

where k is the subgrade modulus in N/m^3 (lbs/in.^{3}).

Thus, Fig. 2a can exactly model the wall behavior, providing the subgrade modulus is given by:

$$k = \frac{tE_c}{R^2} \tag{9}$$

A more convenient method of simulation, capable of modelling thickness variation of the tank walls and complex loading, is to replace the continuous foundation of Fig. 2a by the discrete system of Fig. 2b, where the tank wall is divided into a number of vertical beam elements whose connecting nodes are supported by lateral pin-ended struts from a rigid foundation.

This system can be solved by simple frame analysis, or relaxation programs. Beam members are given the local vertical bending stiffness properties of the section of wall represented, while strut properties model the radial stiffness of that portion of wall extending midway to adjacent nodes above and below, shown shaded in Fig. 2b, and in detail in Fig. 2c for a tapering wall.

Thus, if unit circumferential wall width is again considered, simulation of hoop stiffness requires:

$$y = \frac{2\,p\,R^2}{(t_1 + t_2)E_c} = \frac{p\,\Delta h\,l_i}{A_i E_i} \tag{10}$$

Hence, if for convenience the strut modulus of elasticity E_i is set equal to E_c, then:

$$\frac{A_i}{l_i} = \frac{(t_1+t_2)}{2R^2}\Delta h \tag{11}$$

Either the cross-sectional area A_i, or the length l_i of the strut (or both), may be varied to obtain the required similitude. Loads applied to the vertical beam must be commensurate with the width of wall adopted for analysis (e.g., unit width in the above development). Vertical bending moments in the tank wall are directly modelled by the moments de-

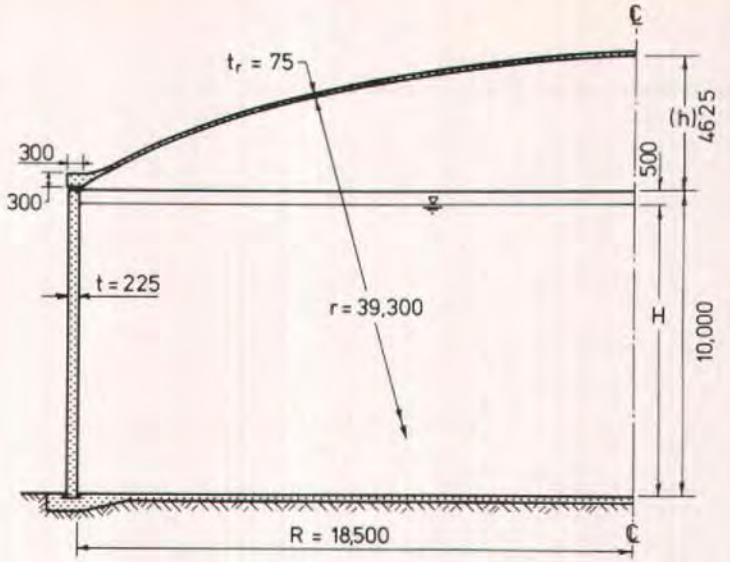

Fig. 3. Example: 10,000 m³ (2.65 million gallon) cylindrical water reservoir. (Note: 1 mm = 0.03937 in.)

veloped in the beam members, and circumferential stresses are found from the node radial displacements, using Eq. (6).

Loading applied to the frame members corresponds to the loads applied to the width of wall modelled, and will generally be applied as resultant joint loads without significant loss of accuracy. Greater accuracy will result by application of the actual distributed loads to the beam members as member loads.

As an example in the use of the frame analogy, the 10,000 m³ (2.65 million gallon) cylindrical water reservoir shown in Fig. 3 is modelled under a 9.5 m (31.2 ft) hydrostatic pressure distribution. Fig. 4a represents the frame simulation, based on ten vertical beam members, modelling a width of 1 m (39.37 in.) in the circumferential direction. Since the wall thickness is constant at 225 mm (8.86 in.), the vertical beam stiffness is:

$$I_b = \frac{1 \times 0.225^3}{12}$$

$$I_b = 0.949 \times 10^{-3} \text{ m}^4 \text{ (2282 in.}^4\text{)}$$

For all except the top strut (i.e., Members 12 to 20 in Fig. 5a), the strut length is arbitrarily chosen as l = 2 m (6.5 ft). Therefore, from Eq. (11):

$$A_t = \frac{2 \times 0.225 \times 1}{18.725^2}$$

$$= 1.283 \times 10^{-3} \text{ m}^2 \text{ (1.99 in.}^2\text{)}$$

For Member 11, to keep member properties the same as Members 12 to 20, the length is increased to 4 m (13 ft), since the tributary wall height is 0.5 m (1.64 ft).

A standard computer program used for routine analysis of structural frames was used to solve the problem, with hydrostatic loading simulated by equivalent joint loads at beam nodes, as shown in Fig. 4a. Results from this simulation are shown plotted as discrete points in Fig. 4b, and compared with results from an analysis using Creasy's tables,[1] which are plotted as continuous curves. Agreement between the two methods is

to within the precision of Creasy's coefficients.

This simple comparison indicates the accuracy of the proposed method for cases that can be modelled by existing tables, and gives confidence in the use of the analogy for load cases that are outside the range of applicability of charts and tables.

PRESTRESS SIMULATION

The frame analogy can also be used to calculate the stresses in the tank walls by prestressing. Consider the case of a tank constructed of precast wall panels, and stressed by tendons in internal ducts as shown in Fig. 5. If F is the tendon force, then the radially inward line load applied to the tank by a single tendon, as shown in Fig. 5a, is:

$$P = F/R \tag{12}$$

The stresses induced by prestress can be found by analyzing the tank wall under the loads P at the appropriate heights, as shown in Fig. 5b. Alternatively, if the spacing s is a small fraction of the wall height, the prestress may be simulated as an equivalent radially inwards pressure of:

$$p = P/s = \frac{F}{Rs} \tag{13}$$

In the case of a tank stressed by wire wrapping, this would be the appropriate approach. However, for a tank prestressed by individual tendons of high prestress force, the local stresses induced by the discrete nature of the prestress line loading may be significant, or the stresses induced during stressing

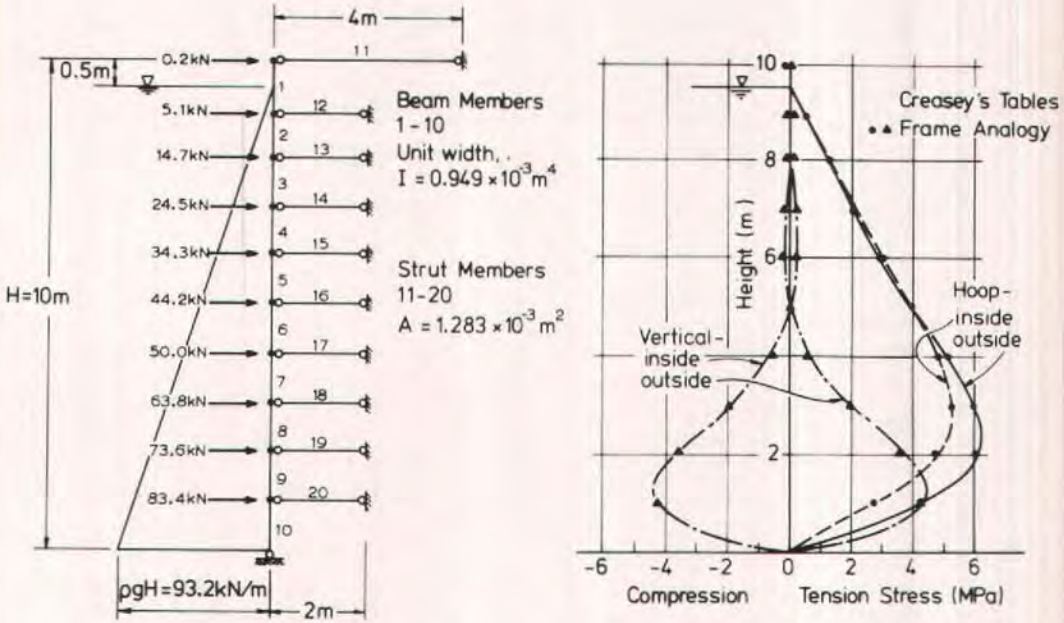

(a) Frame Simulation of Tank in Fig 3

(b) Stresses

Fig. 4. Comparison of stresses under hydrostatic load predicted by frame analogy and Creasy's tables[1] for 10,000 m³ (2.65 million gallon) reservoir.
(Note: 1 m = 39.37 in., 1 MPa = 145 psi.)

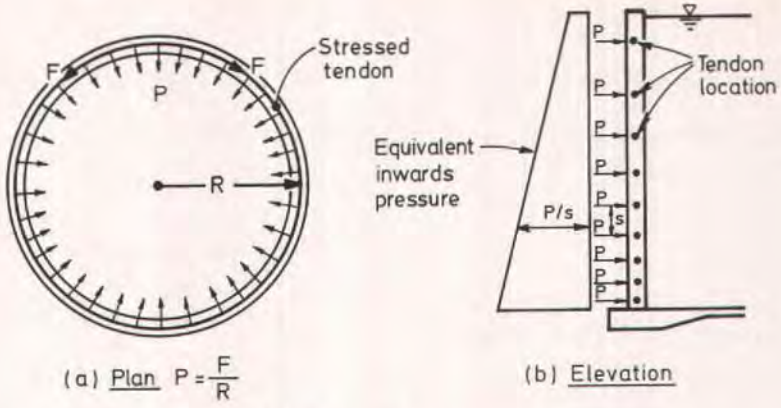

Fig. 5. Forces applied to tank wall by prestressing tendons.

operations by stressing a single tendon may be of interest. In such cases the prestress should be modelled by discrete radial loads to the frame analogy.

As an example of this, the frame simulation of Fig. 4a was used to investigate stresses induced by a tendon located 3.5 m (11.1 ft) above the base and stressed to 860 kN (193.4 kips). From Eq. (12), with R = 18.5 m (60.7 ft), P = 46.5 kN/m (3.19 kips/ft), and for a model representing a unit circumferential length, as in Fig. 4a, this represents the radial load to be applied at the mid-height of Member 7 (see Fig. 4a).

Results from the frame analysis are shown in Fig. 6. Note that the base condition has been assumed pinned, as for the hydrostatic loading. The high local bending stresses resulting from the prestress line load are apparent in Fig. 6, and the Poisson's ratio stresses from the vertical bending have a significant influence on the peak hoop stresses.

It is clear that simulation of prestress as a series of radial loads will provide a more realistic simulation than that provided by an equivalent pressure, using tables or design charts. This method of analysis also enables the prestress design to be optimized since variation in individual tendon positions can be easily modelled.

CREEP DISTRIBUTION OF PRESTRESS

It is common for codes of practice to require a residual compression in the walls of prestressed tanks under fluid loading. This implies a requirement for circumferential prestress at the tank base.

When thermal stresses are considered, the required level of circumferential prestress at the tank base can be as high as 4 to 5 MPa (580 to 725 psi), since it has been shown that circumferential bending stresses of significant magnitude occur due to ambient temperature gradients through the tank wall.[5]

Circumferential precompression cannot be achieved if the prestress is applied with the wall base pinned or fixed, since radial, and hence circumferential strain cannot develop. Consequently, it has been common practice to stress some or all of the circumferential cables with the wall free to slide radially, and then pin the base to improve performance under fluid pressure. This stressing technique is particularly beneficial when tanks are subject to seismic loading.

It is not often recognized that the action of pinning the base after prestress is

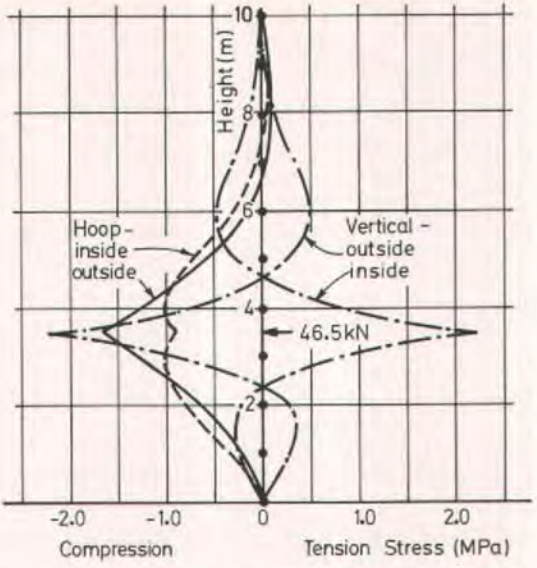

Fig. 6. Stresses induced in 10,000 m^3 (2.65 million gallon) reservoir by single prestressing tendon stressed to 860 kN. (Note: 1 kN = 225 lbs, 1 MPa = 145 psi, 1 m = 39.37 in.)

applied causes a redistribution of prestress due to restraint of creep deflections. Consider the radial deflection of the walls under circumferential prestress, as shown in Fig. 7. If all the prestress is applied with the base free to slide, an initial elastic radially inwards displacement occurs.

If the walls remain free to slide, creep effects would gradually increase the displacements as shown. However, if the base is pinned after stressing, further radial displacement at the base cannot occur, while creep displacements higher up the wall are largely unaffected. The consequence is the development of a radially outwards reaction which will cause vertical bending and a reduction in circumferential prestress at the base.

The problem of creep redistribution due to structural modification can be solved by a rate of creep analysis.[6] The solution indicates that the final behavior can be considered to be identical to that which would result from an elastic analysis considering a portion β_i of the prestress to be applied in the initial structural form (sliding base) with the remainder $\beta_f = 1 - \beta_i$ of the prestress being applied in the modified form (pinned base). From the rate of creep analysis, the following formula can be used:

$$\beta_i = e^{-(\phi_\infty - \phi_\rho)} \tag{14}$$

where ϕ is the creep function set up at time of prestressing, and ϕ_ρ and ϕ_∞ are the values of ϕ at time of pinning the base and after all creep distribution has occurred.

Typically, $\phi_\infty - \phi_\rho \approx 0.9$, giving $\beta_i = 0.40$ and $\beta_f = 0.60$. That is, final prestress will be as though 60 percent of the prestress was applied in the pinned base condition, and only 40 percent in the initial sliding base condition.

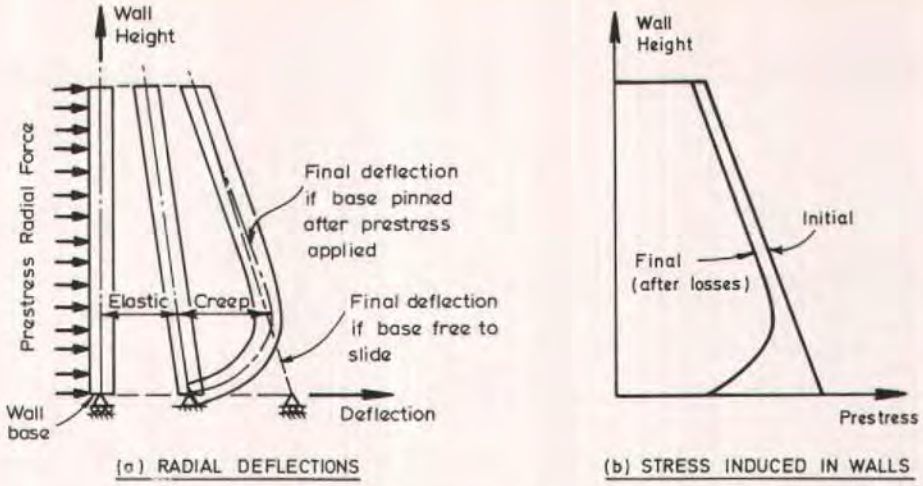

Fig. 7. Redistribution of circumferential prestress due to pinning base after prestressing.

CYLINDRICAL TANKS WITH ROTATIONALLY UNSYMMETRICAL LOADING

It is not commonly realized that loads that are not rotationally symmetric can often be analyzed with adequate accuracy by use of a rotationally symmetric analysis. Of particular interest is the case of seismic loading. Fig. 8 illustrates seismic pressure distributions induced in a cylindrical tank.

The circumferential distribution of pressure follows a cosine distribution with maximum pressure increase and decrease occurring at opposite ends of the diameter parallel to the earthquake excitation. The vertical distribution of pressure on the wall at any location consists of components from impulsive response and convective response (sloshing) of the tank and its contents. Methods for calculating the magnitudes of these pressure distributions have been fully described by Jacobsen[7] and Housner.[8]

For analytical purposes it is common to approximate the curved pressure distributions of Figs. 8b and 8c by linear approximations, as shown. However, it would initially appear that a full shell analysis would be necessary to model the effect of the circumferential variation of pressure. In fact, a solution of sufficient accuracy for maximum stresses may be obtained by assuming the maximum pressure distribution (p_o in Fig. 8a) to be distributed with rotational symmetry around the tank.

This is because at the location of maximum pressure, the rate of variation of pressure in the circumferential direction is small, and stresses induced by shell distortion resulting from pressure differences along adjacent generators are negligible. This being the case, the frame analogy approach or standard design tables or charts may be used to predict maximum stresses induced by earthquake loading.

To provide justification for the above assertion, the cylindrical tank of Fig. 3 was analyzed using Housner's[8] method, for a maximum ground acceleration of 0.4 g. The resulting pressure distribution p_o at the tank generator subjected to maximum pressure increase could be represented with adequate accuracy by

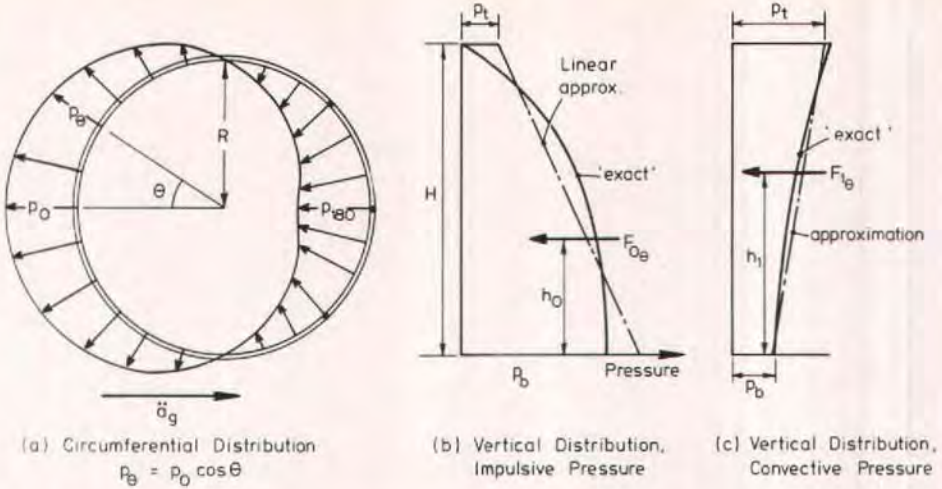

Fig. 8. Seismic pressure distribution in cylindrical tanks.

the linear pressure distribution shown in Fig. 9a, with pressures on a generator at angle θ to the critical generator given by:

$$p_\theta = p_o \cos\theta \qquad (15)$$

The tank was analyzed using the frame analogy simulation of Fig. 4a, assuming the pressure p_o to be constant around the tank circumference, and also by use of a plate bending finite element solution, using the ICES STRUDL PBSQ2 element. The finite element analysis modelled one quadrant of the tank taking advantage of symmetry and antisymmetry about the axes parallel and perpendicular to ground acceleration, respectively, and used 300 rectangular elements (10 up the wall height by 30 round the quarter circumference). The finite element analysis used the same linear vertical pressure distribution at the critical section, but reduced pressure in accordance with Eq. (15) for sections angle θ from the critical section.

Fig. 9b compares results predicted by the full finite element analysis and the frame analogy, for the critical section. The agreement is very close, and certainly justifies the use of the rotational symmetry approximation. The reduction in computer costs, and data preparation and results interpretation in using the simple frame analogy in preference to the finite element analysis is, of course, substantial.

TANKS WITH CURVED GENERATORS

Design tables and charts cannot cover the infinite variety of shapes possible for elevated tanks with curved generators, and sophisticated analytical techniques, such as full shell, or finite element analyses are generally adopted. It is, however, possible to apply the frame analogy simulation, developed above for cylindrical walls, to noncylindrical walls with only minor modification.

Fig. 10 describes the simulation of the bowl of an elevated tank by a frame analogy. In Fig. 10a, the wall is divided into a number of straight meridional beam members, which will carry axial load as well as bending moments and shears. The radial stiffness of the hoop

tension mechanism is again simulated by radial pin-ended struts of equivalent axial stiffness.

In developing the analytical method for cylindrical walls in the previous section, a unit circumferential width of wall was adopted. Consideration of rotational symmetry shows this is inappropriate for noncylindrical walls, and requires use of a slice of constant angle for the full height of the wall. Any angle ϕ may be used, provided loads are also based on the same angular slice.

Beam Properties

Fig. 10b shows a typical beam member ij, of length L_{ij}, and thickness varying from t_i at i to t_j at j. For an angular slice of ϕ radians, the widths at i and j are:

$$b_i = \phi R_i; b_j = \phi R_j \qquad (16)$$

respectively, where R_i and R_j are the radii to the center of the wall at i and j, respectively.

Most computer frame analysis programs allow variation of section properties along the length of a member. However, provided the difference in section between the member ends is not too large, the average properties may be used, namely:

Moment of Inertia:

$$I_{ij} = \frac{1}{12}\left(\frac{b_i+b_j}{2}\right)\left(\frac{t_i+t_j}{2}\right)^3$$

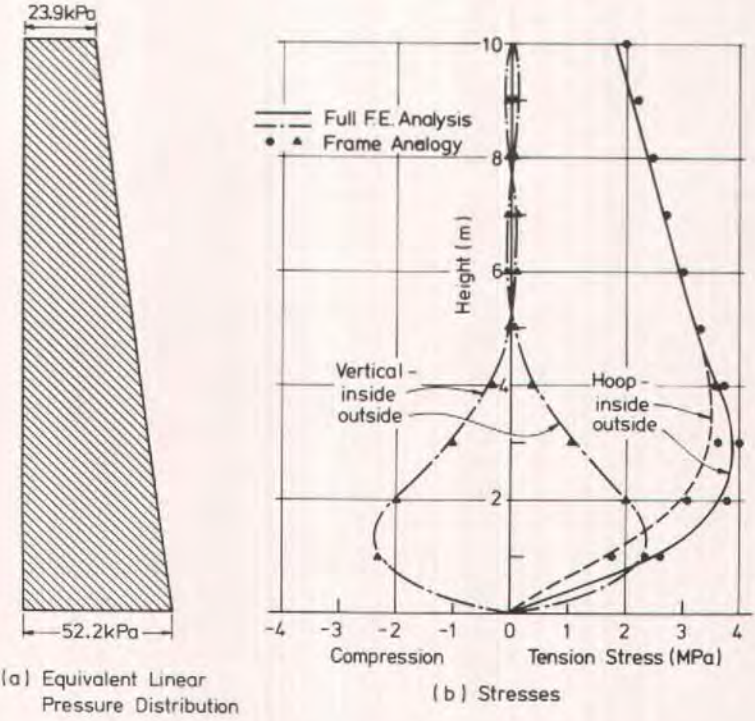

Fig. 9. Seismic stresses for 10,000 m³ (2.65 million gallon) reservoir predicted by frame analogy and full finite element analysis. (Note: 1 kPa = 0.145 psi, 1 MPa = 145 psi, 1 m = 39.37 in.)

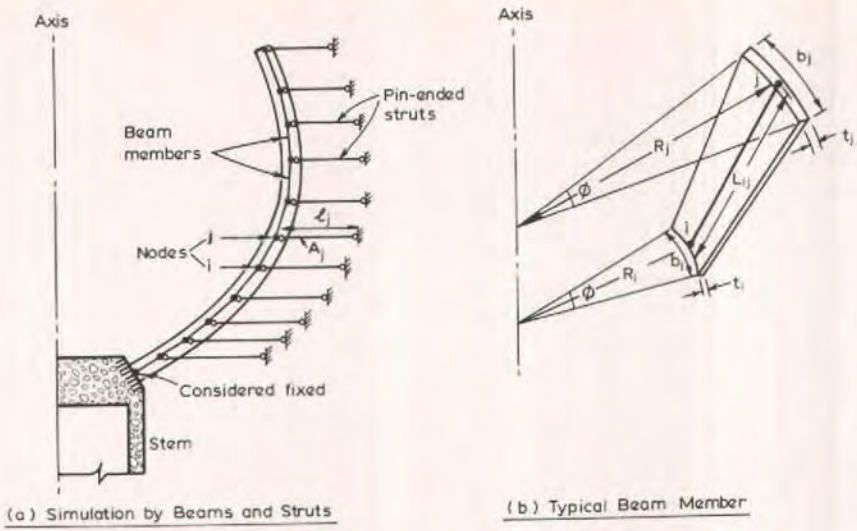

Fig. 10. Frame analogy simulation of noncylindrical elevated tank.

Cross Section Area:

$$A_{ij} = \left(\frac{b_i + b_j}{2}\right)\left(\frac{t_i + t_j}{2}\right) \qquad (18)$$

Note that because of the noncylindrical shape, axial forces will develop in the meridional as well as circumferential directions, making correct simulation of the beam area essential.

Strut Properties

The radial strut j to the node joining adjacent beam members ij and jk must model the circumferential stiffness of half the beam ij and half the beam jk. Putting strut modulus of elasticity equal to that of the walls, the approach used to develop Eq. (11) yields:

$$\frac{A_j}{l_j} = \frac{1}{2}\left[\frac{b_{ij}\, t_{ij}}{R_{ij}^2} \cdot L_{ij} + \frac{b_{jk}\, t_{jk}}{R_{jk}^2} \cdot L_{jk}\right] \qquad (19)$$

where A_j and l_j are the area and length, respectively, of the strut at Node j, and b_{ij}, t_{ij}, R_{ij} are the average width, thickness and radius for Member ij, etc. Note that for $L_{ij} = L_{jk} = \Delta h$; $b_{ij} = b_{jk} = 1$; and $R_{ij} = R_{jk} = R$, Eq. (19) reduces to the value given by Eq. (11) for a unit circumferential width of tapering cylindrical shell.

LOADING

Loads applied to the nodes of a tank simulation, such as those shown in Fig. 10a, must be based on the width of the members adjacent to the nodes. For dead load the simulation is straightforward: provided beam thickness t and width b do not vary excessively between adjoining members, the vertical load P_{vj} at Node j may be approximated as follows:

$$P_{vj} = \frac{1}{2}\,\rho_c\, g\, b_j\, t_j (L_{ij} + L_{jk}) \qquad (20)$$

where $\rho_c g$ is the concrete unit weight.

Loads applied by fluid pressure may be distributed to nodes as shown in Fig. 11a. The distributed load w_{ij} per unit length acts perpendicular to the member axis, thus inducing equivalent forces F_x and F_y at the nodes. The magnitude of w_{ij} depends on member width as well as water head h.

Thus, at Node j:

$$w_j = \rho_f g h_j b_j \qquad (21)$$

where $\rho_f g$ is the fluid unit weight.

Thermal loading requires special consideration, both because of its significance as a stress-inducing load case,[5] and also because of the greater analytical complexity. Figs. 11b and 11c describe a technique for analysis, based on separation of a temperature change through the wall thickness of the tank into an average (uniform) temperature change θ_A, and a differential temperature θ_D, relative to a thermally stress free temperature θ_r, as illustrated in Fig. 12.

The method of analysis is similar to that developed by Priestley[5] for thermal analysis of cylindrical tanks. First, deformations associated with θ_A and θ_D are restrained, and the thermal restraint forces and moments necessary to provide this restraint are calculated (Fig. 11b). Thermal stresses in this restrained condition are calculated. Where the re-

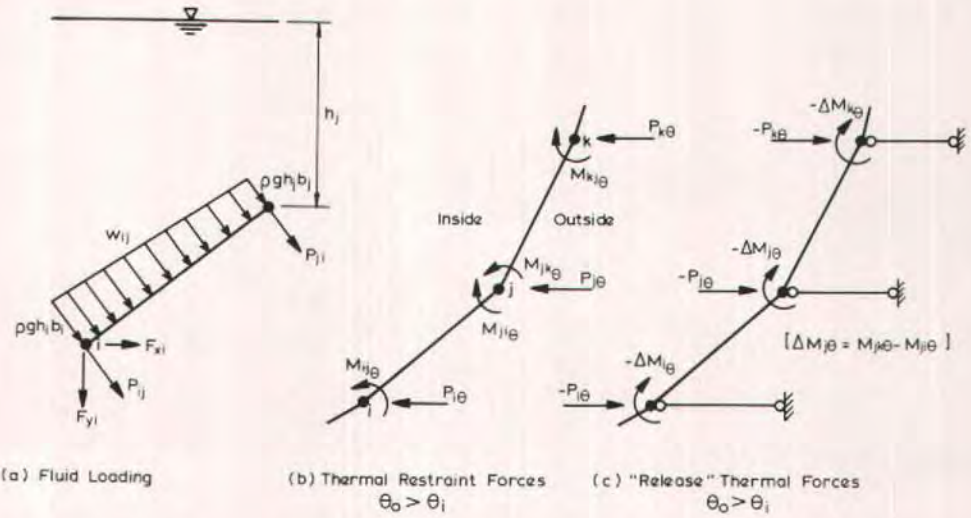

Fig. 11. Equivalent joint loads for frame simulation of elevated tank.

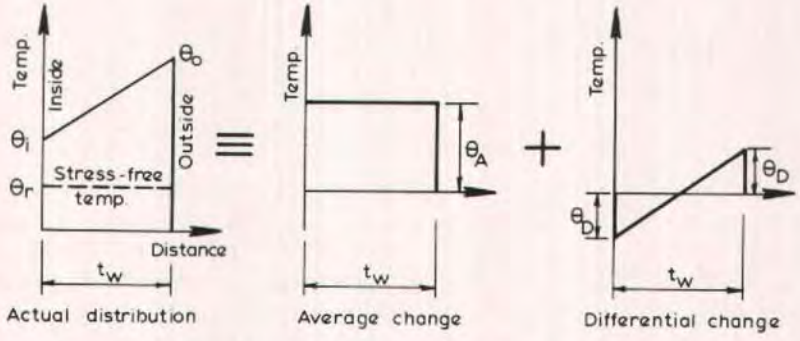

Fig. 12. Components of tank wall temperature change.

straint forces are not balanced by internal equilibrium, equal and opposite release forces must be applied to the structure, and the stresses resulting from analysis under these forces are added to the restraint stresses to obtain the final stress state. The various steps are described in the following.

Step 1— Average Temperature Change: θ_A

Vertical expansion is unrestrained and induces no stress. Restrain the radial thermal expansion associated with θ_A, inducing circumferential compression stress of:

$$f_h = E_c \alpha \theta_A \tag{22}$$

This will require radially inwards restraint forces at the nodes of:

$$P_i = \frac{A_i E_c}{l_i} (\alpha \theta_A R_i) \tag{23}$$

where A_i and l_i are the area and length of the strut at i. These forces are "unbalanced" and will be removed in Step 3.

Step 2 — Differential Temperature Change: θ_D

Restrain circumferential and meridional curvature associated with the differential gradient. Because of the biaxial stress state, this induces circumferential and meridional bending stress of:

$$f_m = f_c = \pm \frac{E \alpha \theta_D}{1-\nu} \tag{24}$$

Assuming average properties for Member ij may be used without excess error, the vertical fixing moments necessary to induce this restraint will be:

$$M_{ij} = M_{ji} = \pm \frac{EI_{ij}\psi}{1-\nu} = \pm \frac{2EI_{ij}\alpha\theta_D}{(1-\nu)t_{ij}} \tag{25}$$

Out of balance moments will occur at joints between members because of different moments of inertia, thickness, and possibly temperature gradient between members. As with cylindrical tanks, the circumferential restraint moments are self-equilibrating.

Step 3 — Release of Restraint Forces

Fig. 11b shows the direction of restraint forces P_i and M_i imposed to restrain the thermal effects resulting from an increase in outside surface temperature relative to inside, and stress-free, temperatures.

These restraint or fixed-end forces must now be released. Forces applied to the structural model to simulate this release are shown in Fig. 11c, that is, the radial restraint loads are reversed in direction, and joint moments $\Delta M_j = -(M_{jk} - M_{ji})$ are applied to joints.

Stresses resulting from analysis under these forces are added to the restraint stresses from the average thermal change [Eq. (22)] and those from restraint of differential thermal change [Eq. (24)], as appropriate, to obtain total thermal stresses.

Where thermal stresses result from diurnal ambient temperature changes in the wall, creep reduction of thermal stress will be negligible. However, when the stress results from storage of hot or cold fluids for considerable periods of time, the magnitude of thermal stress will be appreciably reduced by creep.

Shrinkage and Swelling

The influence of shrinkage and swelling on the stress state in reservoir walls is similar to thermal effects. If the walls shrink due to loss of moisture before filling, there will be a tendency for inward movement which will be restrained at the base, unless it is free to

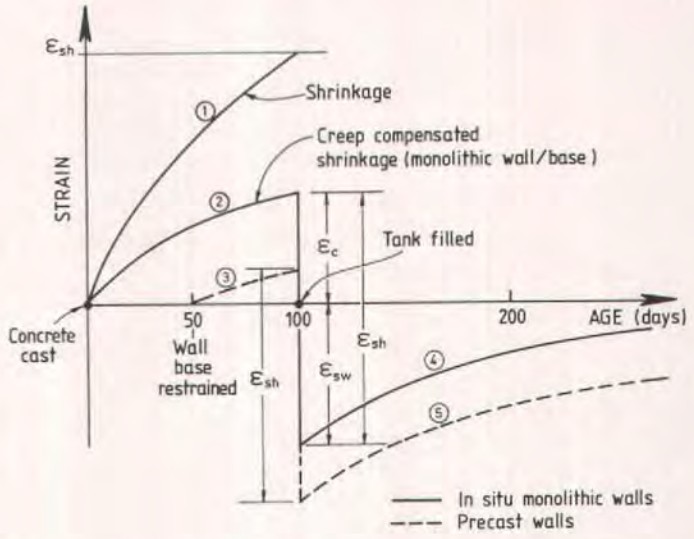

Fig. 13. Effective shrinkage and swelling strains for tank walls.

slide. For circular tanks, restraint will be in the form of a radially outward base reaction inducing hoop tension and vertical bending in the lower parts of the wall.

Since shrinkage develops slowly, the stresses induced are subject to some creep relaxation. Fig. 13 shows the development of shrinkage strain over a period of 100 days after casting, as Line 1. If the wall is monolithically constructed with the base, the creep-compensated (or equivalent elastic) strain is shown by Line 2. A rate of creep analysis[6] gives the creep-compensated strain as:

$$\epsilon_c = \left(\frac{1 - e^{-\phi}}{\phi}\right) \epsilon_{sh} \qquad (26)$$

where ϕ is the value of the creep function at the time considered. If the wall is initially free to slide radially, no stress results from shrinkage until the wall base is pinned, subsequent to stressing. Assuming this occurs when the concrete of the walls is 50 days old, Line 3 represents the development of shrinkage-induced creep-compensated strain (see Fig. 13).

When the tank is filled, the concrete absorbs water and regains its shrinkage very rapidly. The effect is a swelling strain that is again resisted at the base, inducing hoop compressions near the base, and vertical bending moments of opposite sign to those resulting from shrinkage. Although the initial swelling may be considered an elastic strain because it occurs so quickly, the stresses induced are gradually relaxed by creep.

The relationship that applies in terms of equivalent elastic strains, can be shown to be:

$$\epsilon_c' = e^{-\phi'} \epsilon_{sh} \qquad (27)$$

where ϕ' is a new creep factor relating to the age of the concrete at the time of filling the reservoir.

The net effect of shrinkage followed by swelling is illustrated in Fig. 13 by an instantaneous creep-compensated strain change of ϵ_{sh} from Lines 2 to 4, or Lines 3 to 5, followed by a gradual decrease of effective strain.

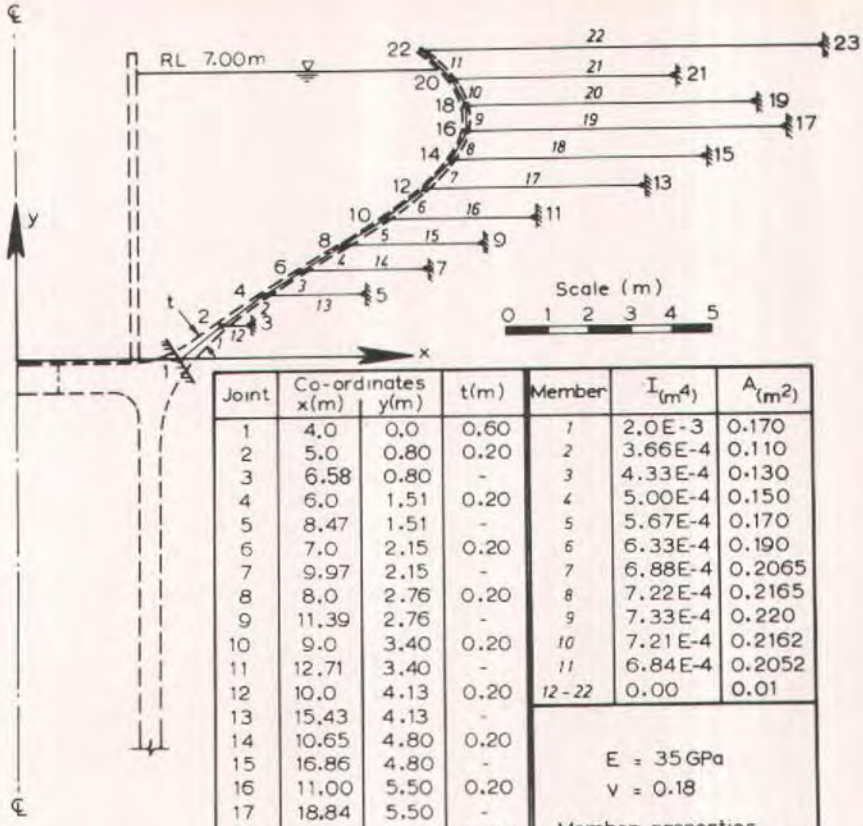

Joint	Co-ordinates x(m)	y(m)	t(m)
1	4.0	0.0	0.60
2	5.0	0.80	0.20
3	6.58	0.80	-
4	6.0	1.51	0.20
5	8.47	1.51	-
6	7.0	2.15	0.20
7	9.97	2.15	-
8	8.0	2.76	0.20
9	11.39	2.76	-
10	9.0	3.40	0.20
11	12.71	3.40	-
12	10.0	4.13	0.20
13	15.43	4.13	-
14	10.65	4.80	0.20
15	16.86	4.80	-
16	11.00	5.50	0.20
17	18.84	5.50	-
18	11.00	6.12	0.20
19	18.14	6.12	-
20	10.62	6.80	0.20
21	16.14	6.80	-
22	9.90	7.50	0.20
23	19.76	7.50	-

Member	$I_{(m^4)}$	$A_{(m^2)}$
1	2.0E-3	0.170
2	3.66E-4	0.110
3	4.33E-4	0.130
4	5.00E-4	0.150
5	5.67E-4	0.170
6	6.33E-4	0.190
7	6.88E-4	0.2065
8	7.22E-4	0.2165
9	7.33E-4	0.220
10	7.21E-4	0.2162
11	6.84E-4	0.2052
12-22	0.00	0.01

E = 35 GPa
ν = 0.18
Member properties based on 0.1 radian slice

Fig. 14. Frame simulation of elevated tank. (Note: 1 m = 39.37 in., 1 GPa = 145,000 psi.)

Stresses induced by these strains may be calculated by analogy to an equivalent average temperature change of:

$$\theta_s = \epsilon_c/\alpha \qquad (28)$$

since both θ_s and ϵ_c will produce identical effects.

Typical values suggested in a recent New Zealand Draft Code[9] for design of concrete water retaining structures, for 200 mm (7.87 in.) precast prestressed walls are 50 x 10^{-6} and 160 x 10^{-6} for effective shrinkage and swelling strains, respectively.

The approach outlined above for thermal stress may be used to calculate the stresses induced in noncylindrical tanks, but for more conventional ground supported cylindrical tanks, published design tables for thermal stresses[5] may be used. Generally, shrinkage stresses will be found to influence only the lower one-quarter of tank wall height and are much less than those resulting from thermal stress.[10]

Table 1. Joint loads for elevated tank in Fig. 14. (Note: 1 kN = 225 lbs, 1 kNm = 738 lb-ft.)

Joint	Water Pressure			Thermal Load		
	FX (kN)	FY (kN)	M (kNm)	FX (kN)	FY (kN)	M (kNm)
2	22.85	−30.34	0	266.0	0	27.10
4	21.72	−32.26	0	84.5	0	−2.86
6	20.75	−33.22	0	82.5	0	−2.86
8	20.67	−33.06	0	82.5	0	−2.86
10	21.61	−31.60	0	84.9	0	−2.82
12	19.58	−23.24	0	64.5	0	−2.35
14	15.50	−11.59	0	60.1	0	−1.45
16	10.78	− 3.23	0	49.1	0	−0.47
18	6.42	1.56	0	53.9	0	0.52
20	2.02	1.21	0	67.4	0	1.57
22	0.02	0.02	0	35.1	0	29.20

EXAMPLE OF USE OF FRAME ANALOGY FOR ELEVATED TANKS

As an example of the use of the frame analogy for tanks of noncylindrical shape, the elevated prestressed concrete reservoir of Fig. 14 was simulated and analyzed under hydrostatic, thermal and prestress loading. For simplicity, the bowl alone was analyzed, and was considered fixed at Joint 1 (see Fig. 14), though a more detailed simulation could have included the bowl base, internal 3 m (39.4 in.) radius shaft, and main column as well. Full details of the simulation, corresponding to a radial slice of 0.1 radians are included in Fig. 14.

Table 1 included joint loads applied to simulate the effects of hydrostatic water load with the free surface at elevation y = 7.0 m (23 ft), and thermal release forces and moments corresponding to a linear temperature gradient with outside surface at 20°C (68°F) above the inside surface (and stress free) temperature.

Fig. 15 compares radial and vertical displacements under hydrostatic loading predicted by the frame analogy with results from an axisymmetric finite element analysis using the program SAP4[11] with elements corresponding to the frame members 1 to 11 (see Fig. 14). For ease of plotting, the vertical axis of Fig. 15 is the straightened meridional generator of the tank. Displacements are a suitable basis for comparing the methods, since hoop stresses are proportional to radial displacements, and meridional bending stresses are dependent on the curvature of the displacements.

Examination of Fig. 15 reveals very close agreement for radial displacements, and good average agreement for vertical displacements, though peak vertical displacements of the finite element solution exceed the corresponding frame values by up to 4 percent. It should be recognized that the simulation of Fig. 14 is rather coarse, particularly in the upper portion of the bowl where meridional curvature is high, and a simulation with more joints in this region should yield more accurate results.

Fig. 16 plots total thermal stresses

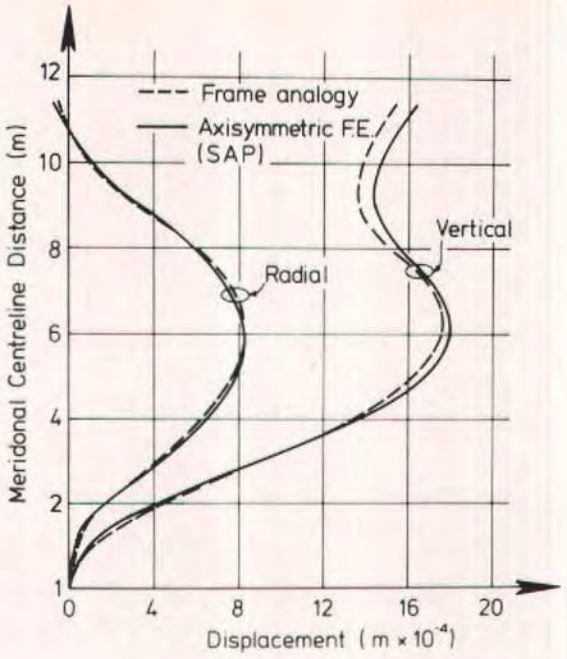

Fig. 15. Displacements of elevated tank (Fig. 14) under hydrostatic loading. (Note: 1 mm = 0.3937 in.)

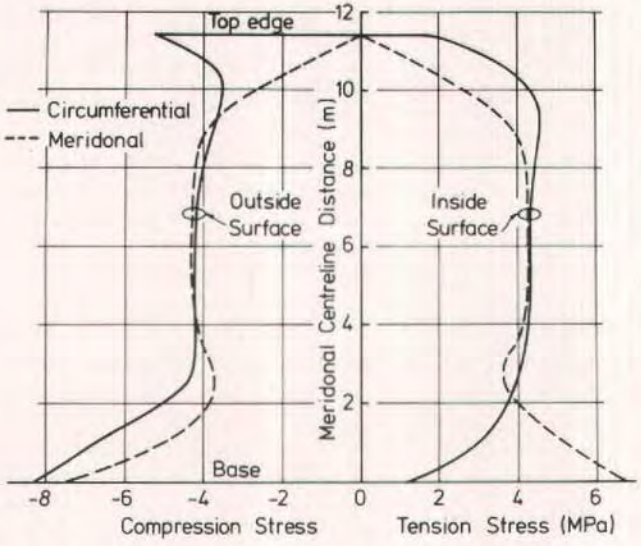

Fig. 16. Thermal stresses for 20°C (68°F) gradient for elevated tank in Fig. 14. (Note: 1 m = 39.37 in., 1°C = 1.8°F, 1 MPa = 145 psi.)

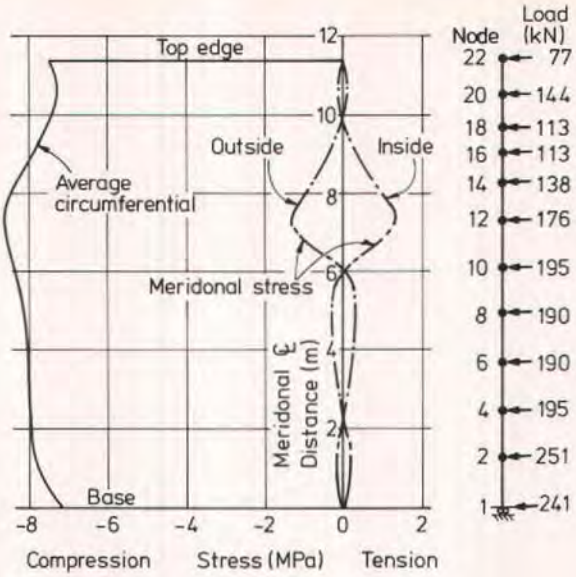

Fig. 17. Circumferential prestress stresses for elevated tank in Fig. 14. (Note: 1 m = 39.37 in., 1 MPa = 145 psi, 1 kN = 255 lbs.)

(i.e., restraint plus release stresses) resulting from analysis under the joint loads of Table 1. The temperature gradient of 20°C (68°F) with the outside surface hotter than the inside is likely to occur frequently as a result of solar radiation on the east or west surface in the early morning or late evening, respectively, and peak gradients are likely to exceed 30°C (86°F).[5]

As with seismic loading, the gradient will not be rotationally symmetric. However, as with seismic loading, errors resulting from analyzing for the critical section as though the local gradient is distributed with rotational symmetry are not particularly significant since the temperature gradient varies only slowly round the circumference. It is perhaps of interest that the stresses induced by the comparatively moderate 20°C (68°F) gradient are substantially higher than those induced by hydrostatic loading.

As a final example, stresses induced in the bowl by circumferential prestressing are examined. It is assumed that the bowl is constructed of precast elements, circumferentially stressed together at ground level, and then lifted up a previously constructed stem by stressing jacks, and fixed to the top of the stem. With this mode of construction, the bowl base will not be radially constrained during the prestressing operation, and circumferential precompression will be induced over the full wall height of the tank.

It is further assumed that the distribution of applied circumferential prestress force up the bowl wall is based on an intended prestress level of 8 MPa (1160 psi) at all heights. It is of interest to investigate the extent to which the double curvature of the bowl redistributes the actual prestress in the walls from the intended level.

Using the frame analogy simulation of Fig. 14, the required nodal loads are found as follows. The circumferential

prestress force F per unit meridional length will be:

$$F = 8t \tag{29}$$

where t is the average shell thickness at the location considered. Hence, from Eq. (13), the equivalent radial pressure will be:

$$\rho = \frac{8t}{R} \tag{30}$$

Thus, at Node j, the radially inwards load will depend on the distance between nodes, and the width of wall simulated:

$$P_j = p \frac{(L_{ij} + L_{jk})}{2} \cdot \frac{(b_{ij} + b_{jk})}{2} \tag{31}$$

$$= \frac{8}{R_j} \cdot \frac{(t_{ij} + t_{jk})}{2} \cdot \frac{(L_{ij} + L_{jk})}{2} \cdot \frac{(b_{ij} + b_{jk})}{2} \tag{32}$$

To analyze under the changed base conditions, Joint 1 in Fig. 14 must be released for rotation and x-direction displacement, and a strut member of length 1.18 m (3.87 ft) added at Joint 1 to represent the stiffness of the lower half of Member 1.

The joint loads given by Eq. (32), and the resulting circumferential and meridional stresses are plotted against a straightened meridional generator in Fig. 17. It will be seen that the average circumferential precompression does not vary greatly from the required 8 MPa (1160 psi) over the wall height, though there is a small redistribution of prestress from the top and bottom of the bowl into the stiffer central region of double curvature.

The meridional bending stresses resulting from circumferential prestress are modest. A Poisson's ratio component from these stresses should be added to the average circumferential surface stresses to obtain the circumferential surface stresses induced by the applied prestress.

Note that if the bowl was fixed to the stem before most of the creep associated with prestressing had occurred, arguments presented above about prestress redistribution resulting from structural modification would apply and a reduction in prestress at the base of the bowl could be expected as radial creep deflections were restrained.

CONCLUSIONS

A frame analogy method for simulating circular prestressed concrete tanks was developed and shown by comparison with more sophisticated methods to be able to accurately predict the behavior of such tanks under a wide variety of loading cases. The method is simple to use, and suitable for both cylindrical and noncylindrical (doubly curved) tanks.

Although the method assumes rotational symmetry of both the tank and its loading, a comparison with results predicted by a full finite element analysis under seismic loading, where the pressure distribution varied round the circumference, indicated that the method could be used with adequate accuracy for nonrotationally symmetric loading.

ACKNOWLEDGMENTS

The finite element solutions included in Fig. 7 and Fig. 11 were provided by Dr. J. H. Wood and Drs. P. J. Moss and A. J. Carr, respectively. Their permission to use the results is gratefully acknowledged.

* * *

REFERENCES

1. Creasy, L. R., *Prestressed Concrete Cylindrical Tanks,* John Wiley and Sons, New York, N.Y., 1961.
2. Ghali, A., *Circular Storage Tanks and Silos,* SPON, London, England, 1979.
3. Hetenyi, M., *Beam on Elastic Foundations,* University of Michigan Press, Ann Arbor, Michigan, 1946.
4. Winkler, E., *Theory of Elasticity and Strength* (in German), Prague, Czechoslovakia, 1867, 184 pp.
5. Priestley, M. J.N., "Ambient Thermal Stresses in Circular Prestressed Concrete Tanks," *ACI Journal,* V. 31, No. 10, October 1976, pp. 553-560.
6. Neville, A. M., *Creep of Concrete: Plain, Reinforced and Prestressed,* Pitman, Bath, England.
7. Jacobson, L. J., "Impulsive Hydrodynamics of Fluid Inside a Cylindrical Tank, and of Fluid Surrounding a Cylindrical Pier," *Bulletin,* Seismological Society of America, V. 39, 1949, pp. 189-204.
8. Housner, G. W., "Dynamic Pressures on Accelerated Fluid Containers," *Bulletin,* Seismological Society of America, V. 47, 1957, pp. 15-35.
9. DZ 3106:1984, "Draft Code of Practice for Concrete Structures for the Storage of Liquids," Standards Association of New Zealand, Wellington, 1984.
10. Priestley, M. J. N., Vessey, J., and North, P. J., "Concrete Structures for the Storage of Liquids," *New Zealand Concrete Construction,* V. 29, February 1985.
11. Bathe, K. J., Wilson, E. L., and Peterson, F. E., "SAP IV — A Structural Analysis Program for Static and Dynamic Response of Linear Systems," Earthquake Engineering Research Center, Report No. EERC 73-11, University of California, Berkeley, June 1973.

* * *

NOTE: Discussion of this paper is invited. Please submit your comments to PCI Headquarters by March 1, 1986.

APPENDIX — NOTATION

A_i = cross section area of frame analogy strut
b_i = width of shell corresponding to radial slice ϕ radians
E_c = modulus of elasticity of concrete
E_i = modulus of elasticity of frame analogy strut
f_c = circumferential stress
f_h = average hoop stress
f_m = meridional stress in doubly-curved shell
f_v = vertical stress in cylindrical shell
F = prestress tendon force
h = height, measured down from top edge of shell
I_b = moment of inertia of frame analogy beam
k = subgrade modulus of equivalent Winkler foundation
l_i = length of frame analogy strut
L_{ij} = length of frame analogy beam member for doubly-curved shell
M = moment
p = pressure on tank wall
P = radial line load applied by circumferential tendon to tank wall
P_i = joint load for frame analogy
R_i = radius of tank at Node i
s = spacing between adjacent tendons in tank wall
t = shell thickness
y = radial deflection of tank
α = coefficient of thermal expansion
ϵ_c = creep compensated shrinkage strain
ϵ_h = hoop strain
ϵ_{sh} = unrestrained shrinkage strain
ϕ = angular slice of doubly-curved shell for frame analogy; also creep factor
ψ = unrestrained thermal curvature
ν = Poisson's ratio for concrete
ρ_c = mass density of concrete
ρ_f = mass density of fluid
θ_A = average temperature change of wall from stress-free temperature
θ_D = differential temperature change at surfaces of wall relative to θ_A

* * *